

## **Increased mTOR activation in idiopathic multicentric Castleman disease**

### **S1: Additional Methodological Information**

#### **S1.1: IHC antibodies**

All staining was performed on formalin fixed paraffin embedded slides. IHC staining was performed on a Bond Max automated staining system (Leica Biosystems). The Bond Refine polymer staining kit (Leica Biosystems) was used. The standard protocol was followed with the exception of the primary antibody incubation which was extended to 1 hour at room temperature. IF staining was performed by hand using standard protocols. Where two ab's for the same species were used TSA amplification and stripping was performed for the first ab stained in series. Stained slides were digitally scanned at 20x magnification on an Aperio CS-O or IF slide scanners (Leica Biosystems).

**Table S1.1**

Antibody	Clone	Vendor	Catalog Number	Dilution	Antigen Retrieval	Protocol
pS6(S235/236P)	Poly	Cell Signaling	2211	1:125	E1-20	IHC-Bond Refine
HIF1a	ESEE122	Invitrogen	14910080	1:1K	E2-20	IHC-Bond Refine
p4EBP1	236B4	Cell Signaling	2855T	1:500	E2-20	IHC-Bond Refine
CD45	2B11+PD7	Dako	M0701	1:200	Pressure Cooker pH9	IF
CD19	LECD19	Dako	M729620	1:100	Pressure Cooker pH9	IF
pS6(S235/236P)	Poly	Cell Signaling	2211	1:100	Pressure Cooker pH9	IF
CD138	MI15	Dako	m7228	1:100	Pressure Cooker pH7	IF
CD3	Poly	Dako	A0452	1:100	Pressure Cooker pH7	TSA-IF
MUM1	EPR5635	Abcam	ab124691	1:1K	Pressure Cooker pH9	TSA-IF
CD20cy	L26	Dako	M0755	1:500	Pressure Cooker pH9	IF
CD68	KP1	Dako	M0814	1:100	Pressure Cooker pH9	IF

### **S1.2: Co-Immunofluorescence measurements**

Immunofluorescence (IF) of FFPE sectioned lymph node tissue was performed at the Pathology Core at the Children's Hospital of Philadelphia. Slides were generated at 5µm thickness and scanned at 20x magnification using Aperio IF slide scanner (LeicaBiosystems). Three equally-sized regions of interest (area ~ 300,000 µm<sup>2</sup>) were determined by visual inspection across all conditions for each iMCD-TAFRO patient (*n* = 4). Germinal centers and large staining artifacts (i.e., folds in the tissue, areas of insufficient staining quality) were manually removed from the analysis for representative interfollicular spaces. HALO digital software (Indica Labs; Albuquerque NM) was utilized to develop detection algorithms to quantify pS6 positive cells. Objects of interest were identified using intensity thresholds and size restrictions and confirmed with visual inspection across all conditions. pS6-positive cells were visually inspected for the presence of the counterstain (CD138, CD3, MUM1, CD68, CD20, CD45). The percentages of double-positive cells were determined independently for each region of interest and were averaged to determine the percentages of double-positive cells for each subject.

### **S1.3: Serum Proteomic Quantification and Gene Set Enrichment Analysis**

Gene set enrichment analysis (GSEA) was performed on serum proteomics data.<sup>1</sup> A separate study in submission (S. Pierson et al, manuscript in submission) also included analyses of these proteomic data, but did not include GSEA for pathways significantly different between these two cohorts or mTORC1 specifically. In short, SomaLogic SOMAscan was used to quantify 1,305 serum analytes in 92 iMCD patients and 44 healthy donors. Four iMCD and two healthy donor samples were removed from analysis after failing quality control. GSEA was performed on the remaining 88 iMCD patients and 42 healthy donors and included 1,139 analytes that mapped to a unique gene and passed quality control. Normalized enrichment score was calculated as the actual enrichment score over the mean enrichment scores against all permutations of the data. Given the relatively small number of genes included, false discovery rate (FDR) < 0.25 was considered appropriate.

### **S1.4: Combining effect sizes from p70S6K, p4EBP1, and pS6**

To compare and synthesize the IHC results using three different mTOR effectors calculated the standardized mean difference (SMD) as the effect size. Specifically, we

used Hedges'  $g$  as the effect size for it allows SMD calculation for different sample sizes in comparison and control. And, it utilizes a small sample correction.<sup>2</sup> Our rationale for attempting to synthesize the three effect sizes is that the observations of the different mTOR effectors should be related as they are part of the same pathway.

The average of the three effects was calculated using the Random Effects Model (RE).<sup>3</sup> This model averages synthesizes the average from different observations by assuming that the variance between them is not only due to random chance but also due to an extraneous variance. The model does not assume that the effect sizes are identical but they are at least related.<sup>4</sup> The RE model assumes that the averages of each observation are stochastically spread around a group-average, and its implementation finds an estimate of this group-average along with a confidence interval. It should be mentioned that this is the same model used in meta-analysis synthesis of treatment/exposure effects from measurements carried out in different populations. All analysis was performed using the metaphor package in  $R$ .<sup>5</sup>

### **S1.5: Assessing pS6 staining proportions versus gender and treatment-responses**

We assessed for pS6-positive staining proportions between IL-6-blockade responders versus non-responders. As mentioned in the main text, the lymph node tissues from the 26 iMCD patients were obtained as close to the time of diagnosis as possible. Of the 26, 24 had sufficient clinical data post-diagnosis to obtain sufficient treatment information. Response to anti-IL6-therapy (with or without cortical steroids) was assessed for patients in the ACCELERATE natural history study using a composite clinical and laboratory criteria. An improvement in greater than or equal to 50% of iMCD minor diagnostic criteria between initiation of therapy and discontinuation constituted as a response.

All statistical comparisons mentioned below were performed using compositional analysis, the same analysis described in the main text.

Twenty of the patients were treated with either siltuximab or tocilizumab. Four patients did not receive either. There was no statistical difference in pS6-positive proportions between patients who were later treated with IL-6-blockade and those who were not. Of the twenty patients treated with anti-IL-6 agents, 18 had sufficient clinical information to assess response. Eleven patients had either a complete or a partial response, while seven patients had a stable disease. Between these two groups, Figure 3A, there were no statistically significant differences for any of the lymph node structures, although there were trends for the mantle zones and the whole follicle ( $p = 0.069$ , follicle;  $p = 0.33$ , germinal center;  $p = 0.10$ , mantle zone;  $p = 0.66$ , interfollicular space).

Four patients were treated with sirolimus after not responding to IL-6-blockade. Two responded to mTOR inhibition while two did not. Figure 3B shows the pS6-positive proportion differences between the two groups.

Since all sentinel lymph nodes were taken from breast cancer patients, we tested for an association between pS6 staining and gender of the iMCD patients. The pS6-positive proportions obtained for the 26 iMCD patients were compared between the female ( $n = 16$ ) and male ( $n = 10$ ) patients. No statistically significant differences in pS6-positive proportions were found for any of the lymph node structures. Figure S1C shows the results.

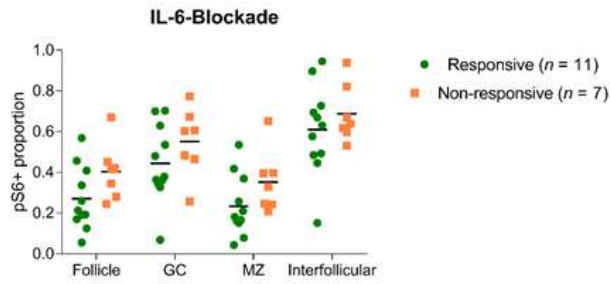
### **S1.6: Flow cytometry**

Samples from iMCD patients and healthy donors were processed following the same protocol. Briefly, cryopreserved cells were thawed, washed with PBS, and stained with a viability dye (LIVE/DEAD Aqua, ThermoFisher) for 10 minutes at room temperature. Cells were then plated in 96-well plates and allowed to rest for 2 hours in serum-free RPMI medium supplemented with 1% penicillin/streptomycin (Lonza). Samples were then treated with cytokine cocktails in a reverse time course. At the end of the time course, samples were fixed on ice immediately with 2% PFA for 20 minutes and permeabilized on ice for 30 minutes with methanol. Cells were then stained overnight, washed, and collected for analysis. Samples were read using a LSRII cytometer (BD Biosciences) and analyzed using FlowJo software (FlowJo, LLC.).

To analyze a statistical difference in the proportion of pS6-positive cells in different cell types (Fig 6A-C: CD14+ monocytes, CD4+ T cells, CD8+ T cells), we performed two-way ANOVA compositional analysis using time and iMCD/healthy-control membership as the two factors. For specific times, we also calculated if the proportion of pS6-positive cells was higher in iMCD compared to healthy controls (Fig 6A-C in main manuscript), by performing non-paired one-tailed Mann-Whitney tests.

An increase in the pS6-positive proportion between 0 min and 120 min (Fig. 6D-F in main manuscript) was tested using a wilcoxon-signed-rank (paired wilcox) test on the transformed proportions. The change from baseline of the pS6-positive proportion (“delta% pS6+”) was compared from a time after IL-6 stimulation to a time after JAK-inhibition. A wilcoxon-signed-rank test was performed to test significance. (Fig G-I in main manuscript).

A



B

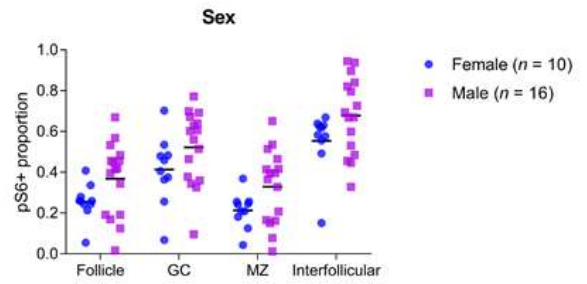


**Figure S1.1 Comparison of pS6-positive stained proportions between gender and treatment responses.** The lymph node tissues were obtained at the time of diagnosis, before treatment was initiated. (A) The proportion of pS6-positive area in each of the regions of lymph node tissue from iMCD patients responsive ( $n = 11$ ) and non-responsive ( $n = 7$ ) to IL-6 blockade with siltuximab or tocilizumab ( $p=0.069$ , follicles;  $p=0.33$ , GC;  $p=0.10$ , MZ;  $p=0.60$ , interfollicular). (B) The proportion of pS6-positive area in each of the regions of lymph node tissue from iMCD patients that are female ( $n = 10$ ) or male ( $n = 16$ ). No significant difference was observed. GC, germinal center; MZ, mantle zone.

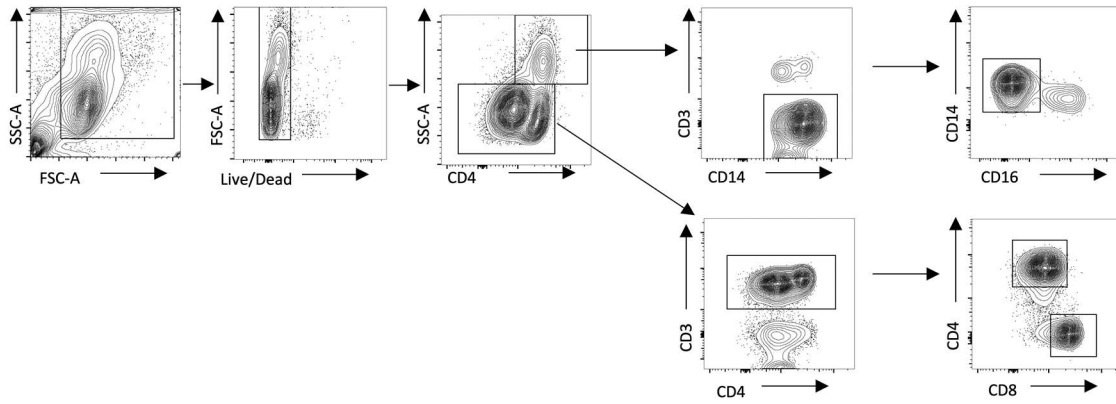


**Figure S1.2 Gating of immune cell populations for analysis in phospho-flow cytometry.** A. Gating of live, singlets followed by identification of CD3- CD14+ monocytes and CD3+ and CD4+ or CD8+ T cells.

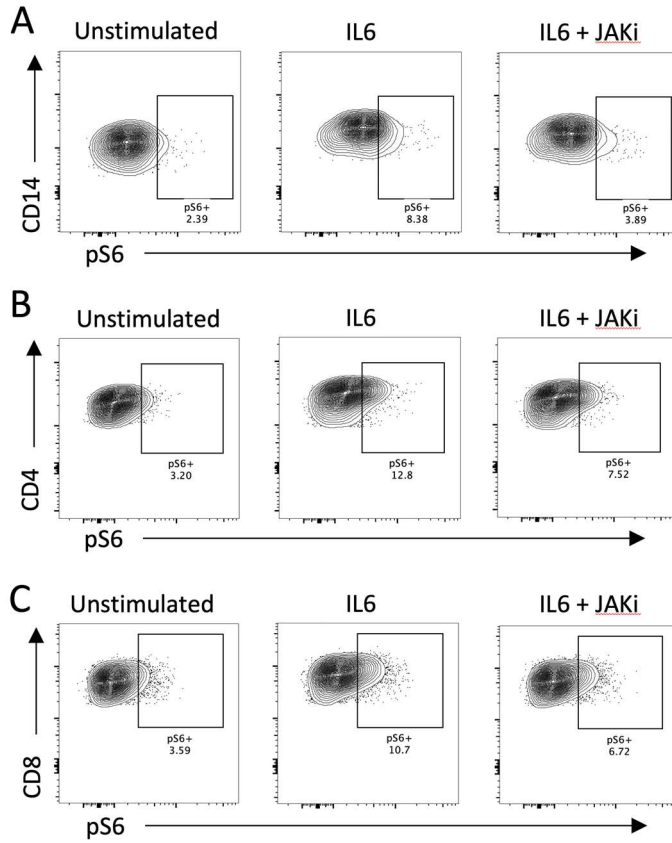


**Figure S1.3 Representative gating of pS6-positive cells from phospho-flow cytometry.** A-C. Representative gating for pS6-positive cells within unstimulated, IL6 treated, or IL6 and JAKi treated CD14<sup>+</sup> monocytes (A), CD4<sup>+</sup> T cell (B), and CD8<sup>+</sup> T cell (C) populations.